

# SCIENTIFIC REPORTS



OPEN

## Human Schwann cells are susceptible to infection with Zika and yellow fever viruses, but not dengue virus

Gaurav Dhiman, Rachy Abraham & Diane E. Griffin

Zika virus (ZIKV) is a re-emerged flavivirus transmitted by *Aedes spp* mosquitoes that has caused outbreaks of fever and rash on islands in the Pacific and in the Americas. These outbreaks have been associated with neurologic complications that include congenital abnormalities and Guillain-Barré syndrome (GBS). The pathogenesis of ZIKV-associated GBS, a potentially life-threatening peripheral nerve disease, remains unclear. Because Schwann cells (SCs) play a central role in peripheral nerve function and can be the target for damage in GBS, we characterized the interactions of ZIKV isolates from Africa, Asia and Brazil with human SCs in comparison with the related mosquito-transmitted flaviviruses yellow fever virus 17D (YFV) and dengue virus type 2 (DENV2). SCs supported sustained replication of ZIKV and YFV, but not DENV. ZIKV infection induced increased SC expression of IL-6, interferon (IFN) $\beta$ 1, IFN- $\lambda$ , IFIT-1, TNF $\alpha$  and IL-23A mRNAs as well as IFN- $\lambda$  receptors and negative regulators of IFN signaling. SCs expressed baseline mRNAs for multiple potential flavivirus receptors and levels did not change after ZIKV infection. SCs did not express detectable levels of cell surface Fc $\gamma$  receptors. This study demonstrates the susceptibility and biological responses of SCs to ZIKV infection of potential importance for the pathogenesis of ZIKV-associated GBS.

Zika virus (ZIKV) is a plus-strand enveloped RNA virus that belongs to the genus *Flavivirus* and is related to other mosquito-borne flaviviruses, including dengue, yellow fever, West Nile, Japanese encephalitis and Spondweni viruses<sup>1</sup>. *Aedes spp.* mosquitoes are the main vectors for ZIKV, yellow fever virus (YFV) and all four types of dengue virus (DENV) but ZIKV can also be transmitted through infected semen and from mother to fetus<sup>2–4</sup>. ZIKV was first isolated from primates in Uganda in 1947, from *Aedes africanus* mosquitoes in 1948<sup>5</sup> and from a febrile man working in Uganda in 1963<sup>6</sup>. For the next five decades sporadic cases of benign, self-limiting acute illness characterized by fever, headache, myalgia and rash were identified in Asia and Africa<sup>7–9</sup>.

The first recognized large outbreak of human ZIKV infection occurred in 2007 on the Pacific island of Yap, in the Federated States of Micronesia<sup>10</sup>. Subsequent outbreaks beginning in October 2013 and continuing throughout 2014 were recognized across Oceania in four groups of Pacific islands: French Polynesia, Easter Island, the Cook Islands, and New Caledonia with 8,750 reported cases<sup>11</sup>. In May 2015, locally acquired ZIKV disease was recognized in Brazil<sup>12</sup> followed by rapid spread through the Americas and Caribbean islands with accompanying reports of neurological complications and congenital malformations including microcephaly<sup>13–15</sup>.

The first association of ZIKV infection with Guillain-Barré syndrome (GBS) was a retrospective study of the French Polynesian outbreak where there was a 20-fold increase in GBS incidence and all of the 42 patients hospitalized with GBS had anti-ZIKV antibody<sup>16</sup>. During the ZIKV outbreak in South America, 66 of the 68 patients with GBS in Colombia had symptoms compatible with ZIKV infection before the onset of GBS<sup>17</sup> and in Martinique, a prospective study determined that the incidence rate of GBS during the 2016 ZIKV outbreak was 4.52 times that of prior years<sup>18</sup>. In 2016, the World Health Organization officially recognized ZIKV as a cause of GBS and microcephaly<sup>19</sup>.

GBS, a potentially life-threatening peripheral nerve disease, is characterized by a rapid onset of bilateral weakness progressing to paralysis that may be accompanied by sensory symptoms. GBS typically occurs 1–3

W. Harry Feinstone Department of Molecular Microbiology and Immunology, Johns Hopkins Bloomberg School of Public Health, 615 North Wolfe Street, Baltimore, MD, 21205, USA. Gaurav Dhiman and Rachy Abraham contributed equally. Correspondence and requests for materials should be addressed to D.E.G. (email: [dgriff6@jhu.edu](mailto:dgriff6@jhu.edu))

weeks after an infectious disease postulated to trigger a pathogen-specific immune response that cross-reacts with peripheral nervous system (PNS) antigens<sup>20</sup>. The most common subtypes of GBS are acute motor axonal neuropathy (AMAN) and acute inflammatory demyelinating polyneuropathy (AIDP), differentiated by the site of immune-mediated injury<sup>21</sup>. In AMAN, membranes of the nerve axon are the primary targets of cross-reactive anti-ganglioside antibodies while in AIDP the Schwann cell (SC)-produced myelin sheath is the target for damage but the relative roles and specificities of antibody and cellular immune responses are unclear<sup>20</sup>.

Several studies have sought to determine the type of GBS associated with ZIKV infection. Although *in silico* comparison of the ZIKV protein sequence with human proteins has identified shared peptides<sup>22</sup>, there is no evidence of disease-relevant cross reactivity so the pathogenesis of ZIKV-associated GBS remains unclear. The electrophysiological findings from the French Polynesian GBS cases were reported to be compatible with the AMAN subtype of GBS, but the typical AMAN-associated anti-ganglioside antibodies were rarely detected<sup>16</sup>. In Colombia, nerve-conduction studies and electromyography were consistent with the AIDP subtype of GBS<sup>17</sup> and the electrophysiologic findings from Martinique were also consistent with AIDP further suggesting that SCs were the target for ZIKV-associated damage<sup>18</sup>.

SCs develop from neural crest cells, are the myelinating glial cells of the PNS and play a central role in peripheral nerve function, maintenance and repair. The SC myelin sheath enables saltatory conduction of action potentials by large diameter axons but SCs also ensheath and maintain axons that are not myelinated. In response to nerve injury SCs can trans-differentiate into a proliferating cell capable of secreting inflammatory mediators that enhance macrophage-mediated myelin removal<sup>23</sup> and can initiate and regulate local immune responses<sup>24,25</sup>. For instance, SCs can be induced to express MHC class I and II molecules, inflammatory cytokines (e.g. TNF $\alpha$ , IL-1 $\beta$ , IL-6, LIF, IL-12, IL-18), chemokines (e.g. CCL2, CCL3, CXCL10) and nitric oxide synthase (iNOS) in response to damage or toll-like receptor (TLR) stimulation<sup>26–29</sup>. Induction of cytokines, chemokines and cell surface immunoregulatory proteins by infection of SCs could promote development of potentially damaging virus- or host cell-specific immune responses.

Because GBS is associated with ZIKV infection and often occurs when symptoms of ZIKV infection are still present and ZIKV RNA is detectable, it has been postulated that GBS might be directly associated with ZIKV infection of peripheral nerve cells or the immune response to viral antigens expressed by these cells<sup>17,30–32</sup>. To evaluate the potential for direct ZIKV-induced peripheral nerve damage, we assessed the susceptibility of immortalized primary human Schwann cells (hSCs)<sup>33</sup> to infection with strains of ZIKV from Africa, Asia and Brazil. Infection with ZIKV was compared to infection with flaviviruses YFV 17D and DENV2 that are less commonly associated with GBS<sup>34,35</sup>. All strains of ZIKV and YFV, but not DENV2, replicated well in hSCs and induced innate responses and cytopathic effect.

## Results

### Human Schwann cells are more susceptible to infection with ZIKV and YFV than DENV.

Immortalized hSCs express SC-characteristic proteins (e.g. S100B), transcription factors (e.g. Slug, TWIST), cell surface receptors (e.g. p75NTR), chemokines (e.g. CCL2) and neurotrophic factors (e.g. NGF, BDNF, NT-3) and can myelinate axons *in vitro*<sup>36</sup>, but have not been evaluated for susceptibility or response to virus infection. To determine susceptibility of hSCs to flavivirus infection, cells were incubated (MOI = 5) with YFV 17D, DENV2 and three strains of ZIKV: 1968 Nigeria, 2014 Thailand and 2015 Brazil (Fortaleza) chosen to represent the historical shifts of ZIKV as it moved from Africa to Asia and finally the Americas<sup>37</sup>. Supernatant fluids, collected from 0 to 120 h after infection, were analyzed by plaque assay (ZIKV, Fig. 1A) or focus forming assay (YFV and DENV, Fig. 1B). The three ZIKV strains replicated well with the highest virus production by ZIKV Brazil (Fortaleza) that peaked at 48 h and continued through 120 h (Fig. 1A). YFV 17D also replicated in hSCs, but DENV2 infection resulted in little virus production (Fig. 1B).

To further evaluate the effects of ZIKV, YFV and DENV infection of hSCs, cells were stained for expression of viral protein and visualized by immunofluorescence microscopy 24–96 h after infection (Fig. 1C). Percentages of cells remaining in the cultures that were infected were quantified (Fig. 1D) and cell viability was determined by MTT metabolism (Fig. 1E) and trypan blue exclusion (Fig. 1F). The percentages of cells expressing detectable viral protein at 48 h when there is little cytopathic effect were: ZIKV Fortaleza 10.7%; ZIKV Nigeria 9.5%; ZIKV Thailand 6.5%; DENV 3.0%; and YFV 12.5%. At 72 and 96 h the numbers of cells in cultures infected with ZIKV Fortaleza, ZIKV Thailand and YFV were greatly diminished (Fig. 1F) and most of the remaining cells were infected (Fig. 1D). Individual ZIKV and YFV-positive cells showed more extensive expression of viral proteins than DENV2-infected cells (Fig. 1C).

To evaluate the response of hSCs to flavivirus infection, cell viability was determined using the MTT mitochondrial function (Fig. 1E) and trypan blue exclusion cell permeability assays (Fig. 1F). Infection at a low MOI of 0.1 for the MTT assay showed significant cell death at 96 h for all three strains of ZIKV and YFV but not DENV2. Infection at a higher MOI of 5 for the trypan blue assay showed evidence of cell death in ZIKV Fortaleza-infected cells at 24 h ZIKV Thailand-infected cells at 48 h, while many ZIKV Nigeria-infected cells were viable 96 h after infection. Cell death was most extensive for YFV-infected cells and few cells remained by 72 h (Fig. 1D,F) and most of the remaining cells were infected (Fig. 1D). Therefore, hSCs were similarly susceptible to evolutionarily distinct ZIKV strains with the Brazilian strain producing the most virus and the African strain the least cytopathic effect. However, hSCs were comparatively resistant to infection with DENV2.

### ZIKV Fortaleza and YFV infections of human Schwann cells induced expression of innate responses.

Interferon (IFN) is an important regulator of cell susceptibility to infection. To determine the responses of hSCs to ZIKV Fortaleza and YFV 17D infection, which had similar levels of replication and similar response (Fig. 1), we analyzed expression of mRNAs for IFN and other IFN pathway proteins (Fig. 2). Levels of mRNAs for IFN $\beta$ 1 and IFN response gene proteins Mx1, a GTPase induced by type I and type III IFNs<sup>38</sup>,

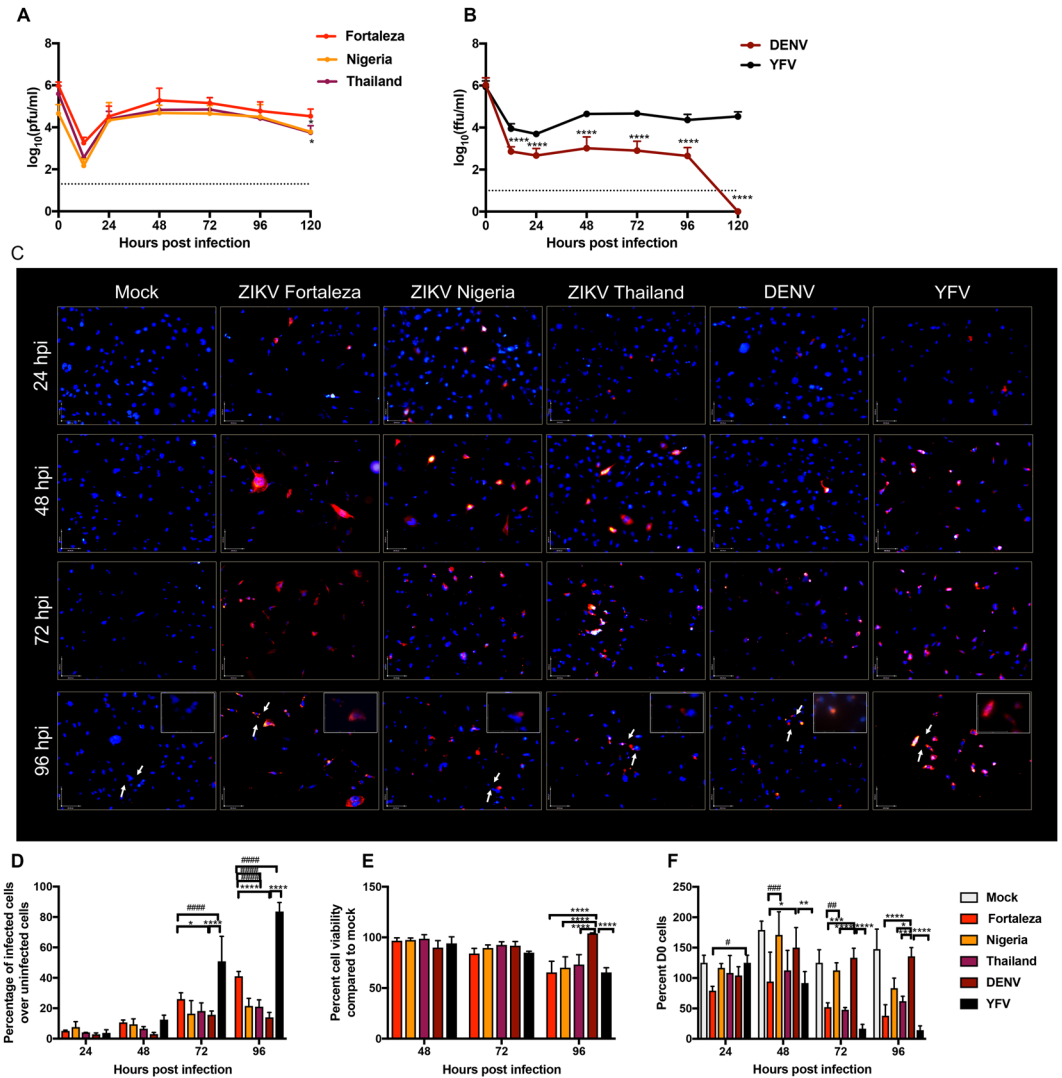


**Figure 1.** - Replication of ZIKV strains 1968 Nigeria (IBH 30656), 2014 Thailand (SCV0127/14) and 2015 Brazil (Fortaleza), YFV (17D) and DENV2 (NGC) in immortalized human Schwann cells. **(A)** hSC cells were infected with strains of ZIKV from Africa (Nigeria), Asia (Thailand) and Brazil (Fortaleza) (MOI = 5). Virus production was measured by plaque formation in Vero cells. Each value represents the average  $\pm$  standard deviation from three independent experiments. \* $P < 0.05$  (Fortaleza vs Nigeria/Thailand). **(B)** hSC cells were infected with DENV2 and YFV (MOI = 5). Virus production was measured by focus formation in Vero cells. Each value represents the average  $\pm$  standard deviation from three independent experiments \*\*\*\* $P < 0.0001$  (DENV vs YFV). **(C)** Immunofluorescence images of mock, ZIKV Fortaleza, ZIKV Nigeria, ZIKV Thailand, DENV, and YFV infected hSCs at 24–96 h after infection (MOI = 5). Cells were stained with pan flavivirus 4G2 antibody followed by anti mouse Alexafuor594 (red). Nuclei were stained with DAPI (blue). The insets show a higher magnification of infected cells (400X). **(D)** The number of infected cells (red) as a percentage of total cells remaining in the culture (blue). Each value represents the average  $\pm$  standard deviation from three different fields. \* $P < 0.05$  \*\*\*\* $P < 0.0001$  DENV vs Fortaleza/YFV, \*\*\*\* $P < 0.0001$  Fortaleza vs Nigeria/Thailand/DENV/YFV **(E)** hSC viability after infection with three strains of ZIKV, YFV and DENV (MOI = 0.1) as determined by MTT assay. Readings taken at 570 nm were plotted as a percentage of the value for mock-infected cells. Each value represents the average  $\pm$  standard deviation from four independent infections. \*\*\*\* $P < 0.0001$  (DENV vs Fortaleza/Nigeria/Thailand/YFV) **(F)** hSC viability after infection with three strains of ZIKV, YFV and DENV (MOI = 5) as determined by trypan blue exclusion. Each value represents the average  $\pm$  standard deviation from three independent experiments of the numbers of viable cells compared to d0 expressed as a percentage. \* $P < 0.05$ , \*\* $P < 0.01$ , \*\*\* $P < 0.001$ , \*\*\*\* $P < 0.0001$  (DENV vs Fortaleza/Nigeria/Thailand/YFV), # $P < 0.05$ , ## $P < 0.01$ , ### $P < 0.001$  (Fortaleza vs Nigeria/YFV).

and IFN-induced protein with tetratricopeptide repeats (IFIT)-1 were upregulated after infection with both YFV and ZIKV with the greatest response induced by YFV. However, IFN  $\beta$ 1 protein production was detectable only in ZIKV Fortaleza-infected cells ( $119 \pm 18.9$  pg/ml at 72 h) (Fig. 2B). IFN $\lambda$ 1 (IL-29) was highly induced in ZIKV-infected hSCs at 48 h after infection and in YFV-infected hSCs at 48 h and 72 h (Fig. 2A). ZIKV infection

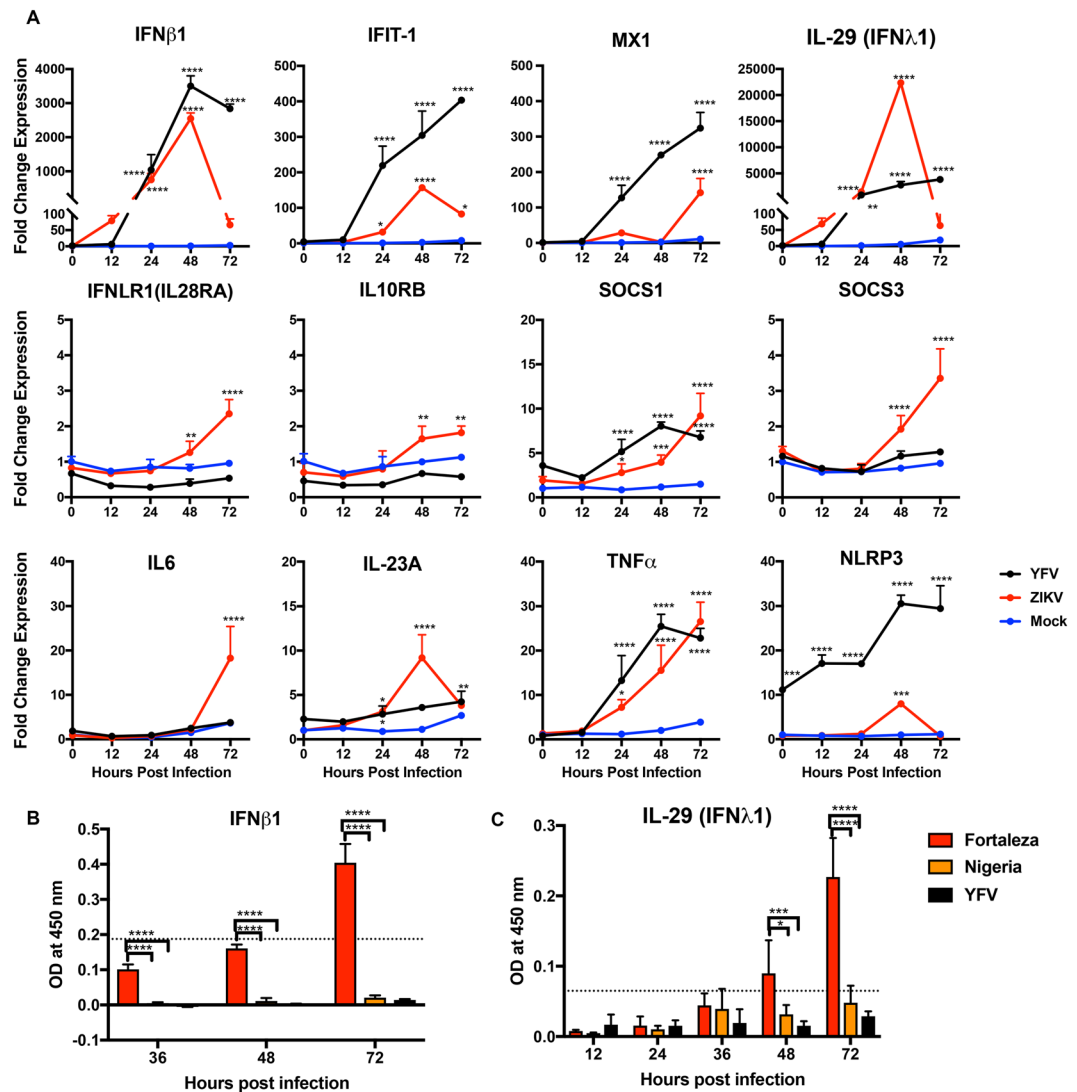


**Figure 2.** Expression of immune response protein mRNAs and proteins induced by ZIKV and YFV infection of human Schwann cells. **(A)** hSC cells were infected with ZIKV Fortaleza and YFV (17D) (MOI = 5) and mRNA expression was measured by qRT-PCR. ZIKV-infected cells (red) and YFV-infected cells (black) were compared to mock-infected cells (blue).  $C_T$  values were normalized to *Gapdh* and fold change was calculated relative to uninfected 0-hour ( $\Delta\Delta C_T$ ) data. Each value represents the average  $\pm$  SD from three independent experiments \* $P < 0.05$ , \*\* $P < 0.01$ , \*\*\* $P < 0.001$ , \*\*\*\* $P < 0.0001$  (mock vs infected). **(B,C)** hSC cells were infected with ZIKV (Fortaleza and Nigeria) and YFV (17D) (MOI = 5) and supernatant fluids were collected. Levels of IFN $\beta$ 1 **(B)** and IFN $\lambda$ 1/IL-29 **(C)** protein were measured by EIA and optical density was plotted. Data are presented as the mean  $\pm$  SD for three independent infections. \* $P < 0.05$ , \*\*\* $P < 0.001$ , \*\*\*\* $P < 0.0001$  (Fortaleza vs YFV/Nigeria).

also increased expression of mRNAs for both IFNLR1 and IL10RB components of the IFN $\lambda$  heterodimeric receptor complex and the SOCS1 and SOCS3 negative regulators of IFN signaling<sup>39</sup>. The levels of IFN $\lambda$ 1 (IL-29) protein at 24 and 36 h were similar, but at 48 and 72 h ZIKV Fortaleza-infected cells produced more IFN $\lambda$ 1 (Fig. 2B). At 48 h protein levels for ZIKV Fortaleza-infected cells were  $37.8 \pm 10.8$  pg/ml and at 72 h were  $75.2 \pm 16.4$  pg/ml for ZIKV Fortaleza and 11.05 pg/ml for ZIKV Nigeria.

To determine whether ZIKV or YFV upregulates hSC expression of other innate response gene mRNAs, levels of mRNAs for representative innate cytokines interleukin (IL)-6, IL-23A and tumor necrosis factor (TNF)- $\alpha$  as well as inflammasome protein NLRP3 were measured (Fig. 2). IL-6 and IL-23A, an innate cytokine related to IL-12 that is associated with induction of autoimmunity<sup>40</sup>, were induced only by ZIKV. Expression of TNF $\alpha$  mRNA was induced in both ZIKV and YFV-infected hSCs. The NLRP3 inflammasome protein mRNA was induced by YFV, but only transiently by ZIKV. Therefore, ZIKV Fortaleza and YFV infections induced overlapping, but distinct innate immune responses in hSCs.

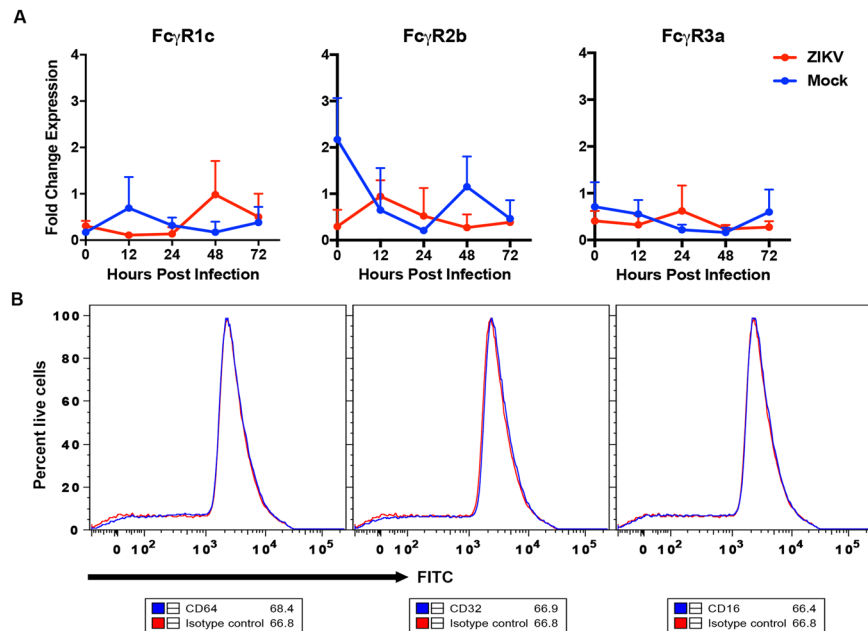


**Figure 3.** Expression of Fc $\gamma$  before and after ZIKV infection of human Schwann cells. **(A)** hSC cells were infected with ZIKV Fortaleza at an MOI of 5 and Fc $\gamma$  receptor mRNA was measured by qRT-PCR. C<sub>T</sub> values were normalized to *Gapdh*, and fold change was calculated relative to uninfected 0-hour ( $\Delta\Delta C_T$ ) data. Each value represents the mean  $\pm$  SD from three independent experiments. **(B)** hSC cells were stained with Fc $\gamma$  receptor-specific antibodies and analyzed by flow cytometry. The blue line in the histogram corresponds to specific staining with the receptor antibody while the red line corresponds to staining with the isotype control antibody. Data are representative of 3 independent sets of experiments.

**Expression of potential receptor and immunomodulatory protein mRNAs by hSCs.** Like other flaviviruses, ZIKV probably can use multiple receptors for host cell attachment, clathrin-mediated endocytosis, pH-dependent membrane fusion and entry<sup>41–43</sup>. Cell surface molecules of potential importance for ZIKV infection include the C-type lectin receptors CD209 (DC-SIGN), CLEC5a and mannose receptor (MR) and the phosphatidyl serine receptors T-cell immunoglobulin and mucin domain (TIM)-1 and TAM receptors Tyro3 and AXL<sup>42–45</sup>. To begin to identify factors that may facilitate flavivirus infection of hSCs, we analyzed expression of mRNAs for protein receptor families reported to mediate entry (Fig. 3). Baseline transcripts were present for heparan sulfate proteoglycan (HSPG2), an attachment protein for many flaviviruses<sup>42</sup>; intercellular adhesion molecule -1 (ICAM-1); MR, a receptor for DENV<sup>46</sup> that colocalizes with MHC class II during phagocytosis by SCs<sup>47</sup>; C-type lectin CD209<sup>48,49</sup>; and TIM1 and TAM receptors<sup>42,50</sup>. We also assessed the modulation of receptor expression during culture and infection. HSPG2 and ICAM-1 mRNA expression increased during culture of hSCs, but this was not affected by ZIKV infection. MR mRNA expression showed a transient increase at 24 h in both infected and uninfected cells. There was little change and no effect of infection on expression of CD209, TIM1, AXL or Tyro3. The intercellular cell adhesion molecule (ICAM-1) a cell surface receptor that can be up regulated by IFN $\gamma$ , IL1 $\beta$  and TNF $\alpha$  in SCs<sup>51</sup> showed increased mRNA expression during culture but was not modulated by ZIKV infection.

**Expression and modulation of functionally important SC protein mRNAs.** Because SC responses to injury can affect peripheral nerve function we also assessed the effect of ZIKV infection on expression of several response-relevant protein mRNAs (Fig. 3). Galectin3 (LGALS3) promotes proinflammatory cytokine expression through the activation of pattern recognition receptor and boosts the phagocytic activity of SCs in injured sciatic nerve in Wallerian degeneration<sup>52</sup>, but levels of mRNA were not modulated by ZIKV infection. Several types of junctional specializations are formed in myelinating SCs between membrane lamellae, act as autotypic junctions and are disrupted during infection of retinal epithelial cells<sup>53,54</sup>. In addition, claudin 1 interacts with the prM protein of DENV to facilitate entry<sup>55,56</sup>. Therefore, we assessed expression of mRNAs for claudins (CLDN) 6 and 9, occludin (OCLN) and zona occludens (ZO)-1. CLDN9 was up regulated in ZIKV-infected hSCs, but other junctional protein mRNAs were not affected by infection.

**Expression of Fc $\gamma$  receptors (Fc $\gamma$ R) by hSCs.** Cross-reacting non- or sub-neutralizing antibodies can enhance flavivirus infection of Fc $\gamma$ R-bearing cells by providing a route of infection for virions coated with non-neutralizing antibodies distinct from binding to the virus cellular receptor and endocytosis<sup>57–61</sup>. SCs in peripheral nerves have been reported to express Fc $\gamma$ RII and Fc $\gamma$ RIII<sup>62,63</sup>. To determine whether immortalized hSCs express Fc $\gamma$ R mRNAs and whether expression is modulated by infection, we assessed the levels of Fc $\gamma$ RIc, Fc $\gamma$ RIIb or Fc $\gamma$ RIIIa mRNAs before and after ZIKV infection (Fig. 4A). Baseline transcripts were detected, but

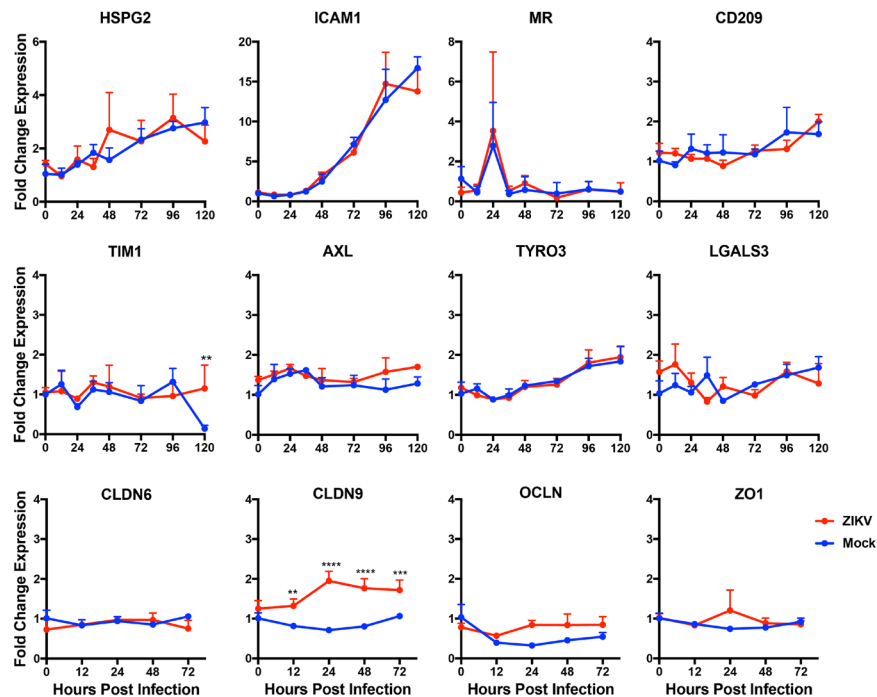


**Figure 4.** Expression of potential flavivirus receptors. hSC cells were infected with ZIKV (Fortaleza) at an MOI of 5 and levels of cellular receptor mRNA were measured by qRT-PCR. Mock-infected cells (blue) were compared to ZIKV-infected cells (red).  $C_T$  values were normalized to *Gapdh*, and fold change was calculated relative to uninfected 0-hour ( $\Delta\Delta C_T$ ) data. Each value represents the average  $\pm$  SD from three independent experiments \*\* $P < 0.01$ , \*\*\* $P < 0.001$ , \*\*\*\* $P < 0.0001$  (mock vs infected).

levels were not affected by ZIKV infection. To determine whether  $Fc\gamma R$  protein was expressed on the cell surface uninfected hSCs were stained with antibodies specific for CD64 ( $Fc\gamma RI$ ), CD32 ( $Fc\gamma RII$ ) and CD16 ( $Fc\gamma RIII$ ) and compared with isotype-specific control antibodies by flow cytometry (Fig. 4B). There was no evidence of  $Fc\gamma R$  expression on the cell surface.

## Discussion

ZIKV was declared a “Public Health Emergency of International Concern” by the World Health Organization because of the neurological complications of infection: microcephaly and GBS<sup>19</sup>. Evidence that ZIKV triggers the AIDP type of GBS that targets SCs suggested the possibility that ZIKV induces GBS by damaging SCs either directly through infection or through the immune response to viral rather than cellular antigens<sup>17,64</sup>. To assess the potential for ZIKV to infect SCs in comparison with other flaviviruses we analyzed the outcome of ZIKV, YFV and DENV interactions with immortalized primary human SCs<sup>33</sup>. SCs were susceptible to infection with evolutionarily distinct strains of ZIKV and to infection with YFV 17D, but not DENV2. SCs responded to infection with increased expression of mRNAs for  $IFN\beta$ ,  $IFN\lambda$ ,  $IFIT-1$ ,  $Mx1$ ,  $NLRP3$ ,  $IL-23A$ ,  $IL-6$  and  $TNF\alpha$ . Baseline transcripts were present for several potential ZIKV receptors and claudin 9 mRNA was increased by infection. hSCs expressed  $Fc\gamma$  receptor mRNAs, but  $Fc\gamma R$  protein was not detected on the cell surface. Therefore, hSCs are susceptible to ZIKV infection and mount a multifaceted innate response, but are unlikely to be targets for antibody-dependent enhanced infection.

There is substantial variation in susceptibility of human cells to flavivirus infection and ZIKV tropism is generally broader than that of DENV<sup>45,65</sup>. The current studies show that hSCs are susceptible to infection with ZIKV and YFV 17D, but not DENV2. Previous *in vitro* studies have shown ZIKV replication in cells from the skin, lung, placenta, muscle, retina, brain, liver, colon, prostate, testes and kidney<sup>43,53,65–68</sup>. Phylogenetic analysis identifies African and Asian lineages of ZIKV with recent outbreaks due to spread of an Asian strain that had acquired mutations potentially relevant to neurovirulence into the Americas<sup>37,69–71</sup>. However, there is limited evidence of strain-specific variation in ZIKV replication *in vitro* or virulence to explain differences in induction of human neurological disease<sup>72</sup>. African strains replicate better than Asian strains in 293 T embryonic kidney cells and neural cells and induce more cell death while Asian strains are more likely to establish persistent infection<sup>66,73,74</sup>. American strains replicate better in placental explants and endothelial cells than African strains<sup>45,75</sup>. In our studies Brazilian ZIKV Fortaleza replicated better and induced more rapid cell death in hSCs than African ZIKV Nigeria.

The 17D vaccine strain of YFV also infects a wide range of human cell types *in vitro*<sup>76,77</sup>. Compared to wild type YFV, YFV 17D infects human cells more efficiently, replicates better and induces more robust activation of innate antiviral responses. Studies of YFV 17D infection of HeLa, 293 T, hepatocyte and dendritic cells have shown induction of  $IFN\beta$ ,  $IL29/IFN\lambda$ ,  $IFIT-1$ ,  $CCL5$  and  $CXCL10$  mRNAs that is dependent on a clathrin-independent, dynamin-dependent mode of entry<sup>76</sup>. Our studies showed that YFV 17D also replicated well in hSCs with virus

production similar to ZIKV (Fig. 1) and induced strong IFN $\beta$ , IFN $\lambda$  and ISG mRNA synthesis (Fig. 2). However, despite efficient *in vitro* replication in SCs, GBS is a rare complication of YFV 17D immunization potentially because *in vivo* spread of the virus is restricted<sup>35,78</sup>.

Flaviviruses can activate pathogen recognition receptors RIG-I, MDA-5, TLR3 and TLR7 to induce expression of IFN and cytokine genes<sup>43,79,80</sup>. The cellular responses of hSCs to ZIKV Fortaleza and YFV 17D infections showed innate antiviral mRNA responses that were similar. Both viruses induced expression of type I and type III IFNs and IFN-stimulated genes (ISGs) IFIT1 and MX1, as previously described for ZIKV infection of A549 respiratory epithelial cells and glomerular podocytes<sup>67,68</sup>. The IFN $\beta$  and ISG response to YFV was greater than to ZIKV, perhaps reflecting the ability of ZIKV to reduce type I IFN induction and NS5 to degrade STAT2 required for IFN signaling<sup>81,82</sup>.

Type III IFN exhibits antiviral and anti-proliferative activities produced through a different receptor but the same downstream signaling pathways as IFN $\alpha$  and IFN $\beta$ <sup>83</sup>. Both ZIKV and YFV-infected cells showed significant increases in IL-29 (IFN $\lambda$ 1) mRNA at 48 h although larger amounts of both IFN $\beta$  and IFN $\lambda$  proteins were produced by ZIKV-infected cells than YFV-infected cells perhaps because of better viability (Fig. 1F). Increased expression of the IFN $\lambda$  heterodimeric receptor complex and negative regulators SOCS1/3 were also observed during ZIKV infection.

The mechanism(s) of ZIKV-induced GBS is not understood. Speculated mechanisms include: Antibody dependent enhancement with DENV sera, an immune mediated mechanism inducing damage through molecular mimicry, cellular mediated inflammation and demyelination induced by complement and macrophage activation, and a direct viral pathogenic effect<sup>64</sup>. Similar mechanisms have been proposed to explain the increased incidence of GBS associated with hepatitis E virus (HEV) infection<sup>84–86</sup>. HEV can replicate in neural cells and virus is often detectable at the onset of GBS, but tropism for SCs has not been examined<sup>87</sup>. Our study of the relationship between ZIKV and GBS, specifically examining hSCs, suggests that GBS could be mediated by pathogen-specific antibodies/T cells or a direct viral effect on SCs rather than cross-reactive antibodies to host proteins/lipids. However, pathologic evaluation of the limited tissue available has not detected ZIKV in peripheral nerves of patients dying with ZIKV-associated GBS<sup>88,89</sup>. The understanding that ZIKV can replicate within hSCs and induces a cellular response that this study demonstrates facilitates a better understanding of the role of ZIKV and GBS in the most recent epidemic.

## Methods

**Cell cultures.** Human SCs, a cell line derived from 60–80 day fetal sciatic nerves and immortalized with SV40 large T antigen and human telomerase reverse transcriptase have been previously described and were obtained from Ahmet Hoke (Department of Neurology, Johns Hopkins School of Medicine)<sup>33,36</sup>. hSCs were grown in Dulbecco's modified Eagle's medium (DMEM; GIBCO Life Technologies) supplemented with 0.2% glucose, 2mM L-glutamine, 10% heat-inactivated fetal bovine serum (FBS), 2  $\mu$ M forskolin, penicillin (100 U/ml) and streptomycin (100  $\mu$ g/ml) at 37 °C in 5% CO<sub>2</sub>. Vero cells (American Type Culture Collection) were grown in DMEM with 10% FBS, 2mM L-glutamine, penicillin and streptomycin at 37 °C in 5% CO<sub>2</sub>. C6/36 *Aedes albopictus* cells (American Type Culture Collection) were grown in DMEM supplemented with 10% FBS and minimal essential amino acids, at 28 °C in 5% CO<sub>2</sub>. Cell viability was determined by trypan blue exclusion.

**Viruses and virus assays.** YFV (17D), DENV2 (NGC) and ZIKV strains 2014 Thailand (SCV0127/14) and 2015 Brazil (Fortaleza) were obtained from Anna Durbin (Johns Hopkins Bloomberg School of Public Health). ZIKV strain 1968 Nigeria (IBH 30656) was obtained from Andrew Pekosz (Johns Hopkins Bloomberg School of Public Health). All virus stocks were grown in C6/36 mosquito cells. Stocks and supernatant fluids from infected cells (MOI = 5) were assayed on Vero cells by focus-formation for DENV and YFV and by plaque-formation for ZIKV. Samples serially diluted in DMEM plus 1% FBS were incubated with Vero cell monolayers for an hour. For focus-forming assays, cells were overlaid with 1% methylcellulose in Optimem (Gibco) with 2% FBS, 2mM glutamine, 50  $\mu$ g/ml gentamicin (Sigma Aldrich) and incubated for 3 days. Cells were fixed with 80% methanol for 10 min, blocked with 5% nonfat milk for 10 min and incubated for 1 h with pan-flavivirus mouse 4G2 monoclonal antibody (purified from hybridoma cells, American Type Culture Collection)<sup>90</sup> diluted 1:2000 in 5% milk followed by horse radish peroxidase-conjugated goat anti-mouse IgG (KPL) diluted 1:3000 in 5% milk for 1 h. Foci were developed with KPL TrueBlue Peroxidase Substrate (Sera Care). For plaque assays, cells were overlaid with 0.6% Bacto Agar in Modified Eagle Medium (MEM, Gibco), incubated for 5 days, fixed with 10% formaldehyde in PBS and stained with 0.2% crystal violet in 20% ethanol.

**MTT cell viability assay.** hSCs were infected with three strains of ZIKV, YFV and DENV (MOI = 0.1). At different times after infection the supernatant fluid was removed and 50  $\mu$ l of MTT reagent (5 mg/ml; thiazolyl blue tetrazolium bromide, Affymetrix USB) in DMEM was added. After 2 h 50  $\mu$ l lysis buffer (20% sodium dodecyl sulfate [Biorad] in 50% N, N'-dimethyl formamide [Applied Biosystems]) was added and incubated for 4 h. Readings at 570 nm were used to calculate the percentage of viable infected cells compared to mock-infected cells.

**Immunofluorescence.** hSCs grown on poly-L-lysine-coated cover slips were infected with the three strains of ZIKV, DENV2 and YFV at a MOI of 5. At 24–96 h after infection, cells were fixed with 4% formaldehyde, permeabilized with 0.2% triton X 100 in PBS, and blocked with 5% normal goat serum in PBS. The cells were incubated with pan-flavivirus 4G2 primary antibody (1:1000 in PBS) for 1 h followed by anti-mouse IgG Alexafluor594 (Invitrogen). Nuclei were stained with DAPI. Images were captured using a Zeiss Axio Imager M2 microscope and analyzed using Volocity software. Numbers of infected and uninfected cells in three fields were counted to determine percentages of cells infected for each virus.

TaqMan Probes (Applied Biosystems)			
Gene	RefSeq.	Taqman Assay ID	
IFNB1	NM_002176	Hs01077958_s1	
IFIT-1	NM_001270929	Hs01675197_m1	
NLRP3	NM_001079821	Hs00918082_m1	
TNF $\alpha$	NM_000594	Hs00174128_m1	
IL-29	NM_172140	Hs00601677_g1	
SOCS1	NM_003745	Hs00705164_s1	
SOCS3	NM_003955	Hs02330328_s1	
MX1	NM_001144925	Hs00895608_m1	
IDT Primers			
Gene	RefSeq.	Forward Primer (5'-3')	Reverse Primer (5'-3')
IL-23A	NM_016584	AGCCGCCCGGGTCTT	TCCTTGAGCTGCTGCCTT TAG
IL6	NM_000600	CCAGCTATGAACCTCTCTC	GCTTGTTCCTCACATCTCTC
IFNLR1	NM_173065	GTAGATGGTCTGGCACTGAG	GATCTGAAGTATGAGGTGGCA
IL10RB	NM_000628	CTCATCCGACAATGGAAGGA	AAGTACGCCTTCTCCCCTA
FCGR1C	NR_027484	TGGAGACCTGCAGTAGTGG	CCCAGCTACAGATCACCTC
FCGR2B	NM_004001	GATTAGTGGGATTGGCTGGTT	GTAGTGGCCTTGATCTACTGC
FCGR3A	NM_001127596	TGGGAGATCAGTCCGCAT	TGAGCTAAATCCGAGGAC
HSPG2	NM_005529	CATAGAGACCGTCACAGCAAG	AGGGCTCGAAATAAACCATC
ICAM1	NM_000201.2	CAATGTGCTATTCAAACCTGCC	CAGCGTAGGGTAAGGTTCTTG
MR	NM_006039.4	GTCATCATTTGTGATCTCCTG	GATGACCGAGTGTTCATCTG
CD209	NM_021155.3	TGGACACTGGGGGAGAGTGG	CATGGCCAAGACACCCTGCT
TIM1	NM_001099414	AACAGATGGGAATGACACCG	GAAGCACCAAGACAGAAATACAG
AXL	NM_001699	TTTATGACTATCTGCGCCAGG	TGTGTCTCCAAATCTTCCCG
TYRO3	NM_006293.3	GCCGCCGAGGCTGAAG	GTCAGGCTCCTCCATCCCCT
LGALS3	NM_002306.3	CTGGGAGATTTGAGGCTCG	TTCCAGACCCAGATAACGC
GAPDH	NM_002046.5	CCATCACTGCCACCCAGAAGAC	GGCAGGTTTTTCTAGACGGCAG
CLDN1	NM_021101	GATTCTATTGCCATACCATGCTG	TGTATGAAGTGCTTGGAAAGACG
CLDN6	NM_021195	GAGACCAGGCCAATCACCC	AATTTCCCTTATCTCCTTCGCA
CLDN9	NM_020982	AAAGCGTCCGTAGCATCTG	GTTTCTGTCTGAGCCTGTT

**Table 1.** Primers used for the study.

**Quantitative real-time RT-PCR (qRT-PCR).** hSCs infected with ZIKV Fortaleza and YFV (MOI = 5) were collected in RLT buffer at 0, 12, 24, 48, and 72 h after infection in triplicate. RNA was isolated from cell lysates using the RNeasy Plus Mini Kit (Qiagen) and quantified using a Nanodrop-1000 spectrophotometer. cDNA was synthesized using the High Capacity cDNA Reverse Transcription Kit (Applied Biosystems) on an Applied Biosystems 2720 thermal cycler with an RNA concentration of 500 ng/ $\mu$ l in a 20  $\mu$ l total reaction volume. qPCR was performed with the Promega GoTaq qPCR Master Mix for Dye-Based Detection using gene-specific oligonucleotide primers for SYBR Green-based measurements or Applied Biosystems TaqMan probes (Table 1). Applied Biosystems 7500 Real Time PCR System was used under the following conditions: initial hold for 2 min at 50 °C and hold for 10 min at 95 °C followed by 40 cycles to denature for 15 s at 95 °C and anneal for 60 s at 60 °C. All gene expression data were normalized against GAPDH levels and fold change compared to uninfected cells was calculated as  $2^{-\Delta\Delta Ct}$ .

**Protein quantification by enzyme immunoassay.** hSCs were infected with ZIKV Fortaleza, YFV and Nigeria and supernatant fluids were collected at 0, 12, 24, 36, 48 and 72 h after infection. IFN  $\beta$  was measured using the VeriKine Human IFN Beta ELISA kit (PBL Assay Science) and IL-29 (IFN $\lambda$ 1) was measured using the Human IL29 Uncoated ELISA kit (Invitrogen) according to the manufacturer's instructions. Supernatant fluids from 3 independent infections were tested and data are presented as pg per ml or OD at 450 nm. Assay range was 50 to 4000 pg/ml for IFN $\beta$  and 15.6 to 1000 pg/ml for IL-29. The limit of detection is marked as the OD value obtained for lowest concentration of assay range.

**Fc $\gamma$  receptor staining.** hSCs were collected in ice cold PBS and live/dead staining (Invitrogen) was done on ice for 30 min in the dark. Cells were stained with FITC-conjugated mouse antihuman CD64 (Fc $\gamma$ RI; BD-560970), CD32 (Fc $\gamma$ RII; ebio 11-0329), CD16 (Fc $\gamma$ RIII; BD-555406) and mouse IgG1 (isotype control; BD-551954) for 1 h on ice and analyzed on a FACSCanto flow cytometer. Histograms were plotted to determine mean fluorescence intensity.

**Statistics.** Data were compared using two-way ANOVA and are presented as mean  $\pm$  standard deviation.  $P < 0.05$  was considered significant. All statistical analyses were performed with GraphPad Prism 5.



## References

- Lanciotti, R. S. *et al.* Genetic and serologic properties of Zika virus associated with an epidemic, Yap State, Micronesia, 2007. *Emerging infectious diseases* **14**, 1232–1239, <https://doi.org/10.3201/eid1408.080287> (2008).
- Abushouk, A. I., Negida, A. & Ahmed, H. An updated review of Zika virus. *Journal of clinical virology: the official publication of the Pan American Society for Clinical Virology* **84**, 53–58, <https://doi.org/10.1016/j.jcv.2016.09.012> (2016).
- Russell, K. *et al.* Male-to-Female Sexual Transmission of Zika Virus—United States, January–April 2016. *Clinical infectious diseases: an official publication of the Infectious Diseases Society of America* **64**, 211–213, <https://doi.org/10.1093/cid/ciw692> (2017).
- Noronha, L., Zanluca, C., Azevedo, M. L., Luz, K. G. & Santos, C. N. Zika virus damages the human placental barrier and presents marked fetal neurotropism. *Mem Inst Oswaldo Cruz* **111**, 287–293, <https://doi.org/10.1590/0074-02760160085> (2016).
- Dick, G. W., Kitchen, S. F. & Haddow, A. J. Zika virus. I. Isolations and serological specificity. *Transactions of the Royal Society of Tropical Medicine and Hygiene* **46**, 509–520 (1952).
- Haddow, A. D. & Woodall, J. P. Distinguishing between Zika and Spondweni viruses. *Bulletin of the World Health Organization* **94**, 711–711A, <https://doi.org/10.2471/BLT.16.181503> (2016).
- Olson, J. G. & Ksiazek, T. G. Suhandiman & Triwibowo. Zika virus, a cause of fever in Central Java, Indonesia. *Transactions of the Royal Society of Tropical Medicine and Hygiene* **75**, 389–393 (1981).
- Fagbami, A. H. Zika virus infections in Nigeria: virological and seroepidemiological investigations in Oyo State. *The Journal of hygiene* **83**, 213–219 (1979).
- Herrera, B. B. *et al.* Continued Transmission of Zika Virus in Humans in West Africa, 1992–2016. *The Journal of infectious diseases* **215**, 1546–1550, <https://doi.org/10.1093/infdis/jix182> (2017).
- Duffy, M. R. *et al.* Zika virus outbreak on Yap Island, Federated States of Micronesia. *The New England journal of medicine* **360**, 2536–2543, <https://doi.org/10.1056/NEJMoa0805715> (2009).
- Ioos, S. *et al.* Current Zika virus epidemiology and recent epidemics. *Med Mal Infect* **44**, 302–307, <https://doi.org/10.1016/j.medmal.2014.04.008> (2014).
- Zanluca, C. *et al.* First report of autochthonous transmission of Zika virus in Brazil. *Mem Inst Oswaldo Cruz* **110**, 569–572, <https://doi.org/10.1590/0074-02760150192> (2015).
- White, M. K., Wollebo, H. S., David Beckham, J., Tyler, K. L. & Khalili, K. Zika virus: An emergent neuropathological agent. *Annals of neurology* **80**, 479–489, <https://doi.org/10.1002/ana.24748> (2016).
- Gatherer, D. & Kohl, A. Zika virus: a previously slow pandemic spreads rapidly through the Americas. *The Journal of general virology* **97**, 269–273, <https://doi.org/10.1099/jgv.0.000381> (2016).
- Pierson, T. C. & Diamond, M. S. The emergence of Zika virus and its new clinical syndromes. *Nature* **560**, 573–581, <https://doi.org/10.1038/s41586-018-0446-y> (2018).
- Cao-Lormeau, V. M. *et al.* Guillain-Barre Syndrome outbreak associated with Zika virus infection in French Polynesia: a case-control study. *Lancet* **387**, 1531–1539, [https://doi.org/10.1016/S0140-6736\(16\)00562-6](https://doi.org/10.1016/S0140-6736(16)00562-6) (2016).
- Parra, B. *et al.* Guillain-Barre Syndrome Associated with Zika Virus Infection in Colombia. *The New England journal of medicine* **375**, 1513–1523, <https://doi.org/10.1056/NEJMoa1605564> (2016).
- Roze, B. *et al.* Guillain-Barre Syndrome Associated With Zika Virus Infection in Martinique in 2016: A Prospective Study. *Clinical infectious diseases: an official publication of the Infectious Diseases Society of America* **65**, 1462–1468, <https://doi.org/10.1093/cid/cix588> (2017).
- Krauer, F. *et al.* Zika Virus Infection as a Cause of Congenital Brain Abnormalities and Guillain-Barre Syndrome: Systematic Review. *PLoS medicine* **14**, e1002203, <https://doi.org/10.1371/journal.pmed.1002203> (2017).
- Willison, H. J., Jacobs, B. C. & van Doorn, P. A. Guillain-Barre syndrome. *Lancet*. [https://doi.org/10.1016/S0140-6736\(16\)00339-1](https://doi.org/10.1016/S0140-6736(16)00339-1) (2016).
- van den Berg, B. *et al.* Guillain-Barre syndrome: pathogenesis, diagnosis, treatment and prognosis. *Nat Rev Neurol* **10**, 469–482, <https://doi.org/10.1038/nrneuro.2014.121> (2014).
- Lucchese, G. & Kanduc, D. Zika virus and autoimmunity: From microcephaly to Guillain-Barre syndrome, and beyond. *Autoimmun Rev* **15**, 801–808, <https://doi.org/10.1016/j.autrev.2016.03.020> (2016).
- Armati, P. J. & Mathey, E. K. An update on Schwann cell biology—immunomodulation, neural regulation and other surprises. *J Neurol Sci* **333**, 68–72, <https://doi.org/10.1016/j.jns.2013.01.018> (2013).
- Meyer zu Horste, G., Hu, W., Hartung, H. P., Lehmann, H. C. & Kieseier, B. C. The immunocompetence of Schwann cells. *Muscle Nerve* **37**, 3–13, <https://doi.org/10.1002/mus.20893> (2008).
- Ydens, E. *et al.* The neuroinflammatory role of Schwann cells in disease. *Neurobiology of disease* **55**, 95–103, <https://doi.org/10.1016/j.nbd.2013.03.005> (2013).
- Lu, M. O. & Zhu, J. The role of cytokines in Guillain-Barre syndrome. *J Neurol* **258**, 533–548, <https://doi.org/10.1007/s00415-010-5836-5> (2011).
- Lee, H. *et al.* Double-stranded RNA induces iNOS gene expression in Schwann cells, sensory neuronal death, and peripheral nerve demyelination. *Glia* **55**, 712–722, <https://doi.org/10.1002/glia.20493> (2007).
- Tzekova, N., Heinen, A. & Kury, P. Molecules involved in the crosstalk between immune- and peripheral nerve Schwann cells. *Journal of clinical immunology* **34**(Suppl 1), S86–104, <https://doi.org/10.1007/s10875-014-0015-6> (2014).
- Spierings, E. *et al.* Mycobacterium leprae-specific, HLA class II-restricted killing of human Schwann cells by CD4+ Th1 cells: a novel immunopathogenic mechanism of nerve damage in leprosy. *Journal of immunology* **166**, 5883–5888 (2001).
- Simon, O. *et al.* Zika virus outbreak in New Caledonia and Guillain-Barre syndrome: a case-control study. *Journal of neurovirology* **24**, 362–368, <https://doi.org/10.1007/s13365-018-0621-9> (2018).
- Roze, B. *et al.* Zika virus detection in urine from patients with Guillain-Barre syndrome on Martinique, January 2016. *Euro surveillance: bulletin Europeen sur les maladies transmissibles = European communicable disease bulletin* **21**, 30154, <https://doi.org/10.2807/1560-7917.ES.2016.21.9.30154> (2016).
- Dirlikov, E. *et al.* Clinical Features of Guillain-Barre Syndrome With vs Without Zika Virus Infection, Puerto Rico, 2016. *JAMA Neurol* **75**, 1089–1097, <https://doi.org/10.1001/jamaneurol.2018.1058> (2018).
- Lehmann, H. C. *et al.* Human Schwann cells retain essential phenotype characteristics after immortalization. *Stem Cells Dev* **21**, 423–431, <https://doi.org/10.1089/scd.2010.0513> (2012).
- Bowman, L. R., Rocklov, J., Kroeger, A., Oliaro, P. & Skewes, R. A comparison of Zika and dengue outbreaks using national surveillance data in the Dominican Republic. *PLoS neglected tropical diseases* **12**, e0006876, <https://doi.org/10.1371/journal.pntd.0006876> (2018).
- McMahon, A. W. *et al.* Neurologic disease associated with 17D-204 yellow fever vaccination: a report of 15 cases. *Vaccine* **25**, 1727–1734, <https://doi.org/10.1016/j.vaccine.2006.11.027> (2007).
- Lehmann, H. C. & Hoke, A. Use of engineered Schwann cells in peripheral neuropathy: Hopes and hazards. *Brain Res* **1638**, 97–104, <https://doi.org/10.1016/j.brainres.2015.10.040> (2016).
- Faria, N. R. *et al.* Zika virus in the Americas: Early epidemiological and genetic findings. *Science* **352**, 345–349, <https://doi.org/10.1126/science.aaf5036> (2016).
- Verhelst, J., Parthoens, E., Schepens, B., Fiers, W. & Saelens, X. Interferon-inducible protein Mx1 inhibits influenza virus by interfering with functional viral ribonucleoprotein complex assembly. *Journal of virology* **86**, 13445–13455, <https://doi.org/10.1128/JVI.01682-12> (2012).

39. Brand, S. *et al.* SOCS-1 inhibits expression of the antiviral proteins 2',5'-OAS and MxA induced by the novel interferon-lambda IL-28A and IL-29. *Biochemical and biophysical research communications* **331**, 543–548, <https://doi.org/10.1016/j.bbrc.2005.04.004> (2005).
40. Langrish, C. L. *et al.* IL-23 drives a pathogenic T cell population that induces autoimmune inflammation. *The Journal of experimental medicine* **201**, 233–240, <https://doi.org/10.1084/jem.20041257> (2005).
41. Rey, F. A., Stiasny, K. & Heinz, F. X. Flavivirus structural heterogeneity: implications for cell entry. *Current opinion in virology* **24**, 132–139, <https://doi.org/10.1016/j.coviro.2017.06.009> (2017).
42. Perera-Lecoin, M., Meertens, L., Carnec, X. & Amara, A. Flavivirus entry receptors: an update. *Viruses* **6**, 69–88, <https://doi.org/10.3390/v6010069> (2013).
43. Hamel, R. *et al.* Biology of Zika Virus Infection in Human Skin Cells. *Journal of virology* **89**, 8880–8896, <https://doi.org/10.1128/JVI.00354-15> (2015).
44. Nowakowski, T. J. *et al.* Expression Analysis Highlights AXL as a Candidate Zika Virus Entry Receptor in Neural Stem Cells. *Cell Stem Cell* **18**, 591–596, <https://doi.org/10.1016/j.stem.2016.03.012> (2016).
45. Liu, S., DeLalio, L. J., Isakson, B. E. & Wang, T. T. AXL-Mediated Productive Infection of Human Endothelial Cells by Zika Virus. *Circ Res*, <https://doi.org/10.1161/CIRCRESAHA.116.309866> (2016).
46. Miller, J. L. *et al.* The mannose receptor mediates dengue virus infection of macrophages. *PLoS pathogens* **4**, e17, <https://doi.org/10.1371/journal.ppat.0040017> (2008).
47. Baetas-da-Cruz, W. *et al.* Schwann cells express the macrophage mannose receptor and MHC class II. Do they have a role in antigen presentation? *J Peripher Nerv Syst* **14**, 84–92, <https://doi.org/10.1111/j.1529-8027.2009.00217.x> (2009).
48. Davis, C. W. *et al.* West Nile virus discriminates between DC-SIGN and DC-SIGNR for cellular attachment and infection. *Journal of virology* **80**, 1290–1301, <https://doi.org/10.1128/JVI.80.3.1290-1301.2006> (2006).
49. Tassaneeritthep, B. *et al.* DC-SIGN (CD209) mediates dengue virus infection of human dendritic cells. *The Journal of experimental medicine* **197**, 823–829, <https://doi.org/10.1084/jem.20021840> (2003).
50. Meertens, L. *et al.* The TIM and TAM families of phosphatidylinositol receptors mediate dengue virus entry. *Cell Host Microbe* **12**, 544–557, <https://doi.org/10.1016/j.chom.2012.08.009> (2012).
51. Lisak, R. P. & Bealmeier, B. Upregulation of intercellular adhesion molecule-1 (ICAM-1) on rat Schwann cells *in vitro*: comparison of interferon-gamma, tumor necrosis factor-alpha and interleukin-1. *J Peripher Nerv Syst* **2**, 233–243 (1997).
52. Mietto, B. S. *et al.* Lack of galectin-3 speeds Wallerian degeneration by altering TLR and pro-inflammatory cytokine expressions in injured sciatic nerve. *Eur J Neurosci* **37**, 1682–1690, <https://doi.org/10.1111/ejn.12161> (2013).
53. Salinas, S. *et al.* Zika Virus Efficiently Replicates in Human Retinal Epithelium and Disturbs Its Permeability. *Journal of virology* **91**, <https://doi.org/10.1128/JVI.02144-16> (2017).
54. Alanne, M. H. *et al.* Tight junction proteins in human Schwann cell autotypic junctions. *J Histochem Cytochem* **57**, 523–529, <https://doi.org/10.1369/jhc.2009.951681> (2009).
55. Che, P., Tang, H. & Li, Q. The interaction between claudin-1 and dengue viral prM/M protein for its entry. *Virology* **446**, 303–313, <https://doi.org/10.1016/j.virol.2013.08.009> (2013).
56. Gao, F. *et al.* Novel binding between pre-membrane protein and claudin-1 is required for efficient dengue virus entry. *Biochemical and biophysical research communications* **391**, 952–957, <https://doi.org/10.1016/j.bbrc.2009.11.172> (2010).
57. de Alwis, R. *et al.* Dengue viruses are enhanced by distinct populations of serotype cross-reactive antibodies in human immune sera. *PLoS pathogens* **10**, e1004386, <https://doi.org/10.1371/journal.ppat.1004386> (2014).
58. Dejnirattisai, W. *et al.* Dengue virus sero-cross-reactivity drives antibody-dependent enhancement of infection with Zika virus. *Nature immunology* **17**, 1102–1108, <https://doi.org/10.1038/ni.3515> (2016).
59. Wahala, W. M. & Silva, A. M. The human antibody response to dengue virus infection. *Viruses* **3**, 2374–2395, <https://doi.org/10.3390/v3122374> (2011).
60. Priyamvada, L. *et al.* Human antibody responses after dengue virus infection are highly cross-reactive to Zika virus. *Proceedings of the National Academy of Sciences of the United States of America* **113**, 7852–7857, <https://doi.org/10.1073/pnas.1607931113> (2016).
61. Ayala-Nunez, N. V. *et al.* How antibodies alter the cell entry pathway of dengue virus particles in macrophages. *Sci Rep* **6**, 28768, <https://doi.org/10.1038/srep28768> (2016).
62. Vedeler, C. A., Scarpini, E., Beretta, S., Doronzo, R. & Matre, R. The ontogenesis of Fc gamma receptors and complement receptors CR1 in human peripheral nerve. *Acta Neuropathol* **80**, 35–40 (1990).
63. Vedeler, C. A., Matre, R., Kristoffersen, E. K. & Ulvestad, E. IgG Fc receptor heterogeneity in human peripheral nerves. *Acta Neurol Scand* **84**, 177–180 (1991).
64. Munoz, L. S., Barreras, P. & Pardo, C. A. Zika Virus-Associated Neurological Disease in the Adult: Guillain-Barre Syndrome, Encephalitis, and Myelitis. *Semin Reprod Med* **34**, 273–279, <https://doi.org/10.1055/s-0036-1592066> (2016).
65. Chan, J. F. *et al.* Differential cell line susceptibility to the emerging Zika virus: implications for disease pathogenesis, non-vector-borne human transmission and animal reservoirs. *Emerg Microbes Infect* **5**, e93, <https://doi.org/10.1038/emi.2016.99> (2016).
66. Simonin, Y. *et al.* Zika Virus Strains Potentially Display Different Infectious Profiles in Human Neural Cells. *EBioMedicine* **12**, 161–169, <https://doi.org/10.1016/j.ebiom.2016.09.020> (2016).
67. Frumence, E. *et al.* The South Pacific epidemic strain of Zika virus replicates efficiently in human epithelial A549 cells leading to IFN-beta production and apoptosis induction. *Virology* **493**, 217–226, <https://doi.org/10.1016/j.virol.2016.03.006> (2016).
68. Alcendor, D. J. Zika Virus Infection of the Human Glomerular Cells: Implications for Viral Reservoirs and Renal Pathogenesis. *The Journal of infectious diseases* **216**, 162–171, <https://doi.org/10.1093/infdis/jix171> (2017).
69. Yuan, L. *et al.* A single mutation in the prM protein of Zika virus contributes to fetal microcephaly. *Science* **358**, 933–936, <https://doi.org/10.1126/science.aam7120> (2017).
70. Haddow, A. D. *et al.* Genetic characterization of Zika virus strains: geographic expansion of the Asian lineage. *PLoS neglected tropical diseases* **6**, e1477, <https://doi.org/10.1371/journal.pntd.0001477> (2012).
71. Gong, Z., Gao, Y. & Han, G. Z. Zika Virus: Two or Three Lineages? *Trends in microbiology* **24**, 521–522, <https://doi.org/10.1016/j.tim.2016.05.002> (2016).
72. Simonin, Y., van Riel, D., Van de Perre, P., Rockx, B. & Salinas, S. Differential virulence between Asian and African lineages of Zika virus. *PLoS neglected tropical diseases* **11**, e0005821, <https://doi.org/10.1371/journal.pntd.0005821> (2017).
73. Ramos da Silva, S., Cheng, F., Huang, I. C., Jung, J. U. & Gao, S. J. Efficiencies and kinetics of infection in different cell types/lines by African and Asian strains of Zika virus. *Journal of medical virology*, <https://doi.org/10.1002/jmv.25306> (2018).
74. Anfasa, F. *et al.* Phenotypic Differences between Asian and African Lineage Zika Viruses in Human Neural Progenitor Cells. *mSphere* **2**, <https://doi.org/10.1128/mSphere.00292-17> (2017).
75. Tabata, T. *et al.* Zika Virus Replicates in Proliferating Cells in Explants From First-Trimester Human Placentas, Potential Sites for Dissemination of Infection. *The Journal of infectious diseases* **217**, 1202–1213, <https://doi.org/10.1093/infdis/jix552> (2018).
76. Fernandez-Garcia, M. D. *et al.* Vaccine and Wild-Type Strains of Yellow Fever Virus Engage Distinct Entry Mechanisms and Differentially Stimulate Antiviral Immune Responses. *mBio* **7**, e01956–01915, <https://doi.org/10.1128/mBio.01956-15> (2016).
77. Liprandi, F. & Walder, R. Replication of virulent and attenuated strains of yellow fever virus in human monocytes and macrophage-like cells (U937). *Archives of virology* **76**, 51–61 (1983).
78. Oliveira, A. C. *et al.* Occurrence of Autoimmune Diseases Related to the Vaccine against Yellow Fever. *Autoimmune Dis* **2014**, 473170, <https://doi.org/10.1155/2014/473170> (2014).

79. Savidis, G. *et al.* The IFITMs Inhibit Zika Virus Replication. *Cell Rep* **15**, 2323–2330, <https://doi.org/10.1016/j.celrep.2016.05.074> (2016).
80. Mandl, J. N. *et al.* Distinctive TLR7 signaling, type I IFN production, and attenuated innate and adaptive immune responses to yellow fever virus in a primate reservoir host. *Journal of immunology* **186**, 6406–6416, <https://doi.org/10.4049/jimmunol.1001191> (2011).
81. Grant, A. *et al.* Zika Virus Targets Human STAT2 to Inhibit Type I Interferon Signaling. *Cell Host Microbe* **19**, 882–890, <https://doi.org/10.1016/j.chom.2016.05.009> (2016).
82. Kumar, A. *et al.* Zika virus inhibits type-I interferon production and downstream signaling. *EMBO Rep*, <https://doi.org/10.15252/embr.201642627> (2016).
83. Kelm, N. E. *et al.* The role of IL-29 in immunity and cancer. *Crit Rev Oncol Hematol* **106**, 91–98, <https://doi.org/10.1016/j.critrevonc.2016.08.002> (2016).
84. van den Berg, B. *et al.* Guillain-Barre syndrome associated with preceding hepatitis E virus infection. *Neurology* **82**, 491–497, <https://doi.org/10.1212/WNL.000000000000111> (2014).
85. Dalton, H. R. *et al.* Hepatitis E virus and neurological injury. *Nat Rev Neurol* **12**, 77–85, <https://doi.org/10.1038/nrneurol.2015.234> (2016).
86. Bazerbachi, F., Haffar, S., Garg, S. K. & Lake, J. R. Extra-hepatic manifestations associated with hepatitis E virus infection: a comprehensive review of the literature. *Gastroenterol Rep (Oxf)* **4**, 1–15, <https://doi.org/10.1093/gastro/gov042> (2016).
87. Zhou, X. *et al.* Hepatitis E Virus Infects Neurons and Brains. *The Journal of infectious diseases* **215**, 1197–1206, <https://doi.org/10.1093/infdis/jix079> (2017).
88. Dirlikov, E. *et al.* Postmortem Findings in Patient with Guillain-Barre Syndrome and Zika Virus Infection. *Emerging infectious diseases* **24**, 114–117, <https://doi.org/10.3201/eid2401.171331> (2018).
89. Ritter, J. M., Martinez, R. B. & Zaki, S. R. Zika Virus: Pathology From the Pandemic. *Arch Pathol Lab Med* **141**, 49–59, <https://doi.org/10.5858/arpa.2016-0397-SA> (2017).
90. Henchal, E. A., Gentry, M. K., McCown, J. M. & Brandt, W. E. Dengue virus-specific and flavivirus group determinants identified with monoclonal antibodies by indirect immunofluorescence. *The American journal of tropical medicine and hygiene* **31**, 830–836 (1982).

## Acknowledgements

These studies were supported by a supplement to research grant R01 NS87539 (D.E.G.) from the U.S. National Institutes of Health. We thank Ahmet Hoke (Johns Hopkins School of Medicine) for the immortalized human Schwann cells and Anna Durbin and Andrew Pekosz (Johns Hopkins Bloomberg School of Public Health) for viruses and reagents used in this study.

## Author Contributions

Experiments were performed by G.D. and R.A. All authors conceived and designed the experiments and wrote the manuscript.

## Additional Information

**Competing Interests:** G.D. and R.A. declare no competing interests. D.E.G. is a member of the Takeda Zika virus vaccine data monitoring committee.

**Publisher's note:** Springer Nature remains neutral with regard to jurisdictional claims in published maps and institutional affiliations.



**Open Access** This article is licensed under a Creative Commons Attribution 4.0 International License, which permits use, sharing, adaptation, distribution and reproduction in any medium or format, as long as you give appropriate credit to the original author(s) and the source, provide a link to the Creative Commons license, and indicate if changes were made. The images or other third party material in this article are included in the article's Creative Commons license, unless indicated otherwise in a credit line to the material. If material is not included in the article's Creative Commons license and your intended use is not permitted by statutory regulation or exceeds the permitted use, you will need to obtain permission directly from the copyright holder. To view a copy of this license, visit <http://creativecommons.org/licenses/by/4.0/>.

© The Author(s) 2019